Published online 18 January 2011

Nucleic Acids Research, 2011, Vol. 39, No. 6 ***e40***
doi:10.1093/nar/gkq1358

A *piggyBac* transposon-based mutagenesis system for the fission yeast *Schizosaccharomyces pombe*

Jun Li[1,2], Jia-Min Zhang[1], Xin Li[1], Fang Suo[1], Mei-Jun Zhang[1], Wenru Hou[1], Jinghua Han[1] and Li-Lin Du[1,*]

[1]National Institute of Biological Sciences, Beijing, 102206 and [2]College of Life Sciences, Beijing Normal University, Beijing 100875, China

Received September 12, 2010; Revised December 25, 2010; Accepted December 28, 2010

ABSTRACT

The TTAA-specific transposon *piggyBac* (*PB*), originally isolated from the cabbage looper moth, *Trichoplusia ni*, has been utilized as an insertional mutagenesis tool in various eukaryotic organisms. Here, we show that *PB* transposes in the fission yeast *Schizosaccharomyces pombe* and leaves almost no footprints. We developed a *PB*-based mutagenesis system for *S. pombe* by constructing a strain with a selectable transposon excision marker and an integrated transposase gene. *PB* transposition in this strain has low chromosomal distribution bias as shown by deep sequencing-based insertion site mapping. Using this system, we obtained loss-of-function alleles of *klp5* and *klp6*, and a gain-of-function allele of *dam1* from a screen for mutants resistant to the microtubule-destabilizing drug thiabendazole. From another screen for *cdc25-22* suppressors, we obtained multiple alleles of *wee1* as expected. The success of these two screens demonstrated the usefulness of this *PB*-mediated mutagenesis tool for fission yeast.

INTRODUCTION

Studies using the model organism *Schizosaccharomyces pombe* have contributed significantly to our understanding of various cellular processes, including cell cycle regulation, genome stability maintenance and cell morphogenesis (1,2). The simplicity of its genome and the ease of genetic manipulations make *S. pombe* one of the most powerful genetic systems (3).

Chemical mutagens such as ethylmethane sulfonate (EMS) and nitrosoguanidine have often been used for mutagenesis in *S. pombe* (4). To map the phenotype-causing mutation, plasmid complementation is a favored approach, but it may require significant efforts if the phenotype needs to be scored clone-by-clone, and it is not suitable for dominant mutations or for certain unstable phenotypes such as epigenetic defects (5). Positional cloning can overcome some of these limitations but is time-consuming despite the availability of sophisticated mapping strains (6). Recently, the next-generation sequencing technique has been applied to mapping chemical-induced point mutations in fission yeast (5). Because more than one mutation is usually introduced during chemical mutagenesis, extensive linkage analysis is still required.

In contrast to chemical mutagenesis, insertional mutagenesis allows mutations to be rapidly identified. Illegitimate recombination-based insertional mutagenesis using a PCR fragment containing a selection marker has been developed for *S. pombe* (7,8). However, multiple and concatemeric integrations of PCR fragments, which are refractory to inverse PCR, may prevent the identification of the sites of integration (9).

Several efforts have been undertaken to develop transposon-mediated mutagenesis tools for *S. pombe*. The endogenous Tf1 retrotransposon was tested but it showed a strong bias against ORFs (10,11). The only transposon so far successfully applied in *S. pombe* is the *Hermes* transposon from *Musca domestica* (12,13).

Transposons do not insert randomly in the genome, which means there are 'cold spots' during mutagenesis if only one transposon is employed (14). A combination of different transposons might provide a solution to reduce insertion bias. For example, a mutagenesis system composed of *P* element and *piggyBac* in *Drosophila melanogaster* was shown to be superior to using a single transposon (15). Therefore, it is worthwhile to develop and utilize multiple transposon-mediated mutagenesis systems in one organism.

piggyBac (*PB*), originally isolated from the cabbage looper moth, *Trichoplusia ni*, has been reported to have mobility in a diverse range of organisms, including the budding yeast *Saccharomyces cerevisiae*, the fruit fly *D. melanogaster*, the zebra fish *Danio rerio* and the mouse *Mus musculus* (16–20). Even though *PB* prefers

*To whom correspondence should be addressed. Tel: +86 10 80713938; Fax: +86 10 80720499; Email: dulilin@nibs.ac.cn

to use TTAA as its target sequence, it has little bias against ORFs, as demonstrated by the work in *D. melanogaster* (15). The broad host range and the low insertion bias make *PB* an attractive mutagenesis tool. Importantly, when *PB* is excised from the genome, the double-stranded break left behind is precisely repaired most of the time, thus rendering it easy to verify whether a transposon insertion has caused a phenotype by conducting a reversion analysis (21–23).

In this study, we developed an inducible *PB* transposition system for *S. pombe*. With this system, we performed two proof-of-principle genetic screens and obtained the expected mutants.

MATERIALS AND METHODS

Plasmid constructs

pPB[ura4] was constructed by replacing the ApaI–SacII fragment of PB[SV40-neo] with an ApaI–SacII fragment containing the *ura4*$^+$ marker from a pBluescript-based plasmid. PB[SV40-neo] was described previously (20).

pREP1-PBase was constructed by cloning a NcoI restriction fragment of CMV-PBase (20), which contains the coding sequence of the *piggyBac* transposase, into the polylinker of pREP1 vector, downstream of the *nmt1* promoter.

Integration plasmid pDUAL-PBase was constructed as follows: a plasmid from the fission yeast ORFeome library (24), pDUAL-Crb2-YFH1c, was digested by BglII and SphI to remove the *nmt1* promoter and the DNA sequences encoding Crb2 and the YFH tag, and then ligated with a restriction fragment containing the *nmt1* promoter and the PBase ORF from pREP1-PBase.

Schizosaccharomyces pombe strains and media

All the strains used in this study were constructed with standard method or isolated upon *PB* transposition (listed in Table 1). DY166 was isolated as a stable Ura$^+$ derivative upon *PB* transposition from pPB[ura4]. Strains with *PB* insertion at the *arg6* and *ade6* loci were derived from DY166 by screening for auxotrophic mutants caused by *PB* transposition upon PBase induction.

Media were prepared according to the standard procedure (4). Thiabendazole (TBZ) was dissolved in DMSO as a stock solution at 20 mg/ml and then added to YES medium at the indicated concentrations. 5-Fluoro-orotic acid (FOA) was used at a concentration of 1 g/l in YE plates consisting of 0.5% yeast extract, 3% glucose and 2% agar. Vitamin B_1 (thiamine) was used in Edinburgh minimal medium (EMM) at a final concentration of 15 μM to repress the *nmt1* promoter.

Transposition induction in *S. pombe*

In the experiments using *PB[ura4*$^+$*]* on an episomal plasmid, Ura$^-$ cells harboring a PBase plasmid were first grown in a medium without thiamine to induce PBase expression. Then the plasmid pPB[ura4] was introduced into the cells by transformation with lithium acetate method and cells were spread on plates lacking uracil.

In the experiments using *PB[ura4*$^+$*]* integrated at *ade6* or *arg6* locus, strains containing both integrated *PB* and *nmt1* promoter-driven PBase were first cultured in liquid EMM medium with proper supplements and thiamine. Then the cells were washed and transferred to EMM without thiamine to allow the expression of PBase. At indicated time points, cells were spread on EMM plates with thiamine but lacking adenine or arginine to monitor the numbers of cells that became Ade$^+$ or Arg$^+$, and on YES plates to monitor the total cell numbers. FOA-resistant derivatives were isolated by transferring cells pre-grown in EMM media without thiamine onto FOA plates.

Inverse PCR for mapping the insertion sites of *PB[ura4*$^+$*]*

Genomic DNA was prepared with MasterPure yeast DNA purification kit (Epicentre Technologies) and digested with HaeIII overnight. After heat inactivation of HaeIII, digested genomic DNA was ligated with T4 DNA ligase at 16°C for 6 h. PCR was performed with two pairs of primers: (i) oligos 12 and 13; (ii) oligos 14 and 15 (Table 2). PCR products were sequenced using oligos 12 or 15 as primers, respectively. All the oligonucleotides used in this study are listed in Table 2.

Quantitative PCR for detecting the copy number of *PB[ura4*$^+$*]*

Purified genomic DNA was analyzed on an ABI Fast 7500 System using the TaKaRa SYBR Green PCR kit according to the manufacturer's instructions. PCR primers were LD252 and LD253 for *act1*$^+$, oligo 69 and oligo 70 for *PB[ura4*$^+$*]*. *PB* copy number was determined by $\Delta\Delta C_T$ method using genomic DNA of strain DY1432 as a control, which has a single copy of *PB* (25). Since the ratios of *PB* versus *act1*$^+$ were usually not integral numbers, we estimated the copy number to be the integral closest to the ratios.

Genetic screens with *PB*

In the screen for TBZ-resistant mutants, DY1434 cells were mutagenized by culturing in the absence of thiamine in EMM medium supplemented with histidine and arginine for ~40 h and then spread on EMM plates containing thiamine and histidine but not arginine to select for Arg$^+$ Ura$^+$ cells (~1 OD600 unit cells for each 9-cm plate). After 20 h at 30°C, EMM plates were replica-plated to YES plates containing 40 mg/l TBZ. TBZ plates were then incubated at 30°C until resistant mutants formed colonies.

In the screen for suppressors of *cdc25-22* at the restrictive temperature, transposition-mediated mutagenesis was performed with strain DY1007 grown at 25°C. After the PBase induction period in liquid medium, cells were spread on EMM plates containing thiamine but not arginine and the plates were incubated at 37°C until visible colonies appeared.

Table 1. Yeast strains used in this study

Strains	Genotype	Sources
DY1010	*h*$^+$ *his3-D1 ura4-D18 leu1-32::leu1*$^+$*::nmt1::*PBase (integration of pDUAL-PBase)	This study
DY166	*h*$^+$ *his3-D1 ura4-D18 leu1-32 PB[ura4*$^+$*]* (TTAA at chromosome 1 coordinate 3749391)	This study
DY319	*h*$^-$ *ura4-D18 leu1-32 ade6::PB[ura4*$^+$*]* (TTAA at chromosome 3 coordinate 1316297)	This study
DY1432	*h*$^-$ *his3-D1 ura4-D18 arg6::PB[ura4*$^+$*]* (TTAA at chromosome 2 coordinate 1229486) *leu1-32::leu1*$^+$*::nmt1::*PBase (integration of pDUAL-PBase)	This study
DY1433	Same as DY1432	This study
DY1434	Same as DY1432	This study
DY1007	*h*$^-$ *his3-D1 ura4-D18 cdc25-22 arg6::PB[ura4*$^+$*] leu1-32::leu1*$^+$*::nmt1::*PBase (integration of pDUAL-PBase)	This study
DY2533	*h*$^-$ *his3-D1 ura4-D18 leu1-32::leu1*$^+$*::nmt1::*PBase (integration of pDUAL-PBase) *ade6::PB[ura4*$^+$*]*	This study
DY3038	*h*$^-$ *his3-D1 ura4-D18 arg6::PB[ura4*$^+$*] leu1-32::leu1*$^+$*::nmt1::*PBase (integration of pDUAL-PBase); a spontaneous mutation leading to TBZ resistance	This study; TBZ-resistant derivative of DY1434
DY3039	*h*$^-$ *his3-D1 ura4-D18 klp6::PB[ura4*$^+$*]* (TTAA at chromosome 2 coordinate 533911) *leu1-32*::leu1$^+$::nmt1::PBase (integration of pDUAL-PBase)	This study; TBZ-resistant derivative of DY1434
DY2552	*h*$^-$ *his3-D1 ura4-D18 klp5::PB[ura4*$^+$*]* (TTAG at chromosome 2 coordinate 1711478) *leu1-32*::leu1$^+$::nmt1::PBase (integration of pDUAL-PBase)	This study; TBZ-resistant derivative of DY1434
DY1542	*h*$^+$ *his3-D1 ura4-D18 arg6::PB[ura4*$^+$*] klp6Δ::kanMX4*	This study; Bioneer strain backcrossed into lab strain background
DY2284	*h*$^-$ *his3-D1 ura4-D18 dam1::PB[ura4*$^+$*]* (TTAA at chromosome 1 coordinate 3106534) *leu1-32*::leu1$^+$::nmt1::PBase (integration of pDUAL-PBase)	This study; TBZ-resistant derivative of DY1434
LD329	*h*$^-$ *his3-D1 ura4-D18*	Lab stock

Table 2. Oligonucleotides used in this study

Name	Sequences (5′–3′)	Use
oligo 12	cctcgatatacagaccgataaaacacatgc	For inverse PCR
oligo 13	agtcagtcagaaacaactttggcacatatc	For inverse PCR
oligo 14	cttgaccttgccacagaggactattagagg	For inverse PCR
oligo 15	cagtgacacttaccgcattgacaagcacgc	For inverse PCR
oligo 69	tcacgcggtcgttatagttc	For qPCR against *PB*
oligo 70	gacgcatgcattcttgaaat	For qPCR against *PB*
LD252	tgctcctcctgagcgtaaatactctgtctg	For qPCR against *act1*$^+$
LD253	aacgataccaggtccgctctcatcatactc	For qPCR against *act1*$^+$
oligo 111	ctgtaagccgccaatcggac	For checking footprints at *ade6* promoter
oligo 112	tgctgcatccaagatgatgc	For checking footprints at *ade6* promoter
oligo 93	ttggatgattgcttgcatgg	For checking insertions in *klp5*
oligo 94	cgtatttgaatatacggacc	For checking insertions in *klp5*
oligo 95	ggcgcgactatggttcatag	For checking insertions in *klp6*
oligo 96	ttcccatacttgtgttcttc	For checking insertions in *klp6*
oligo 106	aatggttctgatcaggacgc	For checking insertions in *klp5*
oligo 107	gcaagcttcgattcatgagc	For checking insertions in *klp5*
oligo 108	cgtggtgagcgtagataggc	For checking insertions in *klp6*
oligo 109	ttagactcttcagcaatcctc	For checking insertions in *klp6*
oligo 128	cctcacgggagctccaagcggcgac	For *PB* insertion sequencing
oligo 498	caagcagaagacggcatacgagatcggtctcggcattcctgctgaacc	For *PB* insertion sequencing
oligo 145	aatgatacggcgaccaccgagatctacactgagcaatatttcaagaatgcatgc	For *PB* insertion sequencing
oligo 496	p-gatcggaagagcggttcagcaggaatgccgag	For *PB* insertion sequencing
oligo 497	acccttctcagcacataccgctcttccgatct	For *PB* insertion sequencing
oligo 549	catgcgtcaattttacgcagactatctttcta	For *PB* insertion sequencing
Seqr	caagcagaagacggcatacga	For *PB* insertion sequencing

Profiling the insertion sites of *PB* with high-throughput sequencing

About 400 000 Arg$^+$ Ura$^+$ colonies derived from DY1432, DY1433 and DY1434 upon transposition induction for 2 days in liquid EMM medium without thiamine were harvested and pooled. Genomic DNA was extracted from 30 OD600 units of cells and fragmented to the size of 250–1000 bp by sonication. The fragmented DNA in the size range of 250–750 bp was purified from 2% agarose gel with GFX PCR DNA and Gel Band Purification Kit (GE Healthcare). A DNA adaptor composed of oligo 496 and 497 was ligated to the DNA fragments with NEBNext DNA Sample Master Mix Set 1 (New England Biolabs). To amplify the *PB* insertion site-flanking sequences, we performed 30 cycles of PCR with a *PB*-specific primer close to the terminal repeats (oligo 128) and a primer annealing to the adaptor (oligo 498). After purification using the GFX kit, a further round of 30-cycle PCR was performed with primers oligo 145 and Seqr to add sequences needed for Illumina sequencing. Forty-two cycle single-end sequencing was

carried out using an Illumina Genome Analyzer II. The sequencing primer oligo 549 was designed such that the first three bases of *PB*-specific reads were GGG from *PB* terminal repeats followed by *PB*-flanking genomic DNA sequence.

About 7 million sequence reads starting with GGG were obtained. After trimming the first three bases from these reads, the remaining 39 bp was mapped to *S. pombe* genome sequence (downloaded from Sanger Center genome database, 15 October 2010 version) with Bowtie version 0.12.7 (26). Only perfectly matched and uniquely mapped reads (~5.3 million) were kept for further analysis. For multiple reads having the same sequence, we conservatively considered them coming from a single insertion event, as read numbers can be strongly influenced by the timing of transposition events during the 2-day induction, the proliferation rates of the cells, and amplification bias during the PCR steps. Insertion site data analyses were carried out using Perl, Matlab and Microsoft Excel. The sequencing data have been deposited at Sequence Read Archive (accession number SRA027355).

RESULTS

PB transposes in fission yeast

To test whether *PB* has mobility in *S. pombe*, we constructed a binary transposition system (Figure 1A). In this binary system, the transposon was provided by the donor plasmid pPB[ura4], in which a *ura4*$^+$ marker was flanked by inverted terminal repeats (ITRs) of *PB*. The transposase PBase under the control of the thiamine-repressible *nmt1* promoter was expressed from a plasmid pDUAL-PBase integrated into chromosome 2 at the *leu1* locus. Strain DY1010 containing the integrated PBase plasmid was cultured in liquid medium without thiamine for ~36 h to induce PBase expression and then was transformed with the donor plasmid pPB[ura4]. Since there is no *S. pombe* autonomous replication sequences (replication origins) in pPB[ura4] and the host strain is uracil auxotrophic, only cells which have integrated the *ura4*-containing sequence into their genome can proliferate robustly on media without uracil. Circular plasmids are not good substrates for recombination and thus rarely get integrated into the genome. As expected, only low levels of Ura$^+$ transformant colonies were observed with a control strain that had no PBase, probably due to the infrequent integration of the whole plasmid (Figure 1B). In contrast, the presence of PBase dramatically increased the transformation frequency (Figure 1B). A similar result was obtained when the PBase was expressed from the episomal plasmid pREP1-PBase (data not shown). If PBase-dependent transformation events happened through transposition, the *PB*-flanking sequences in the Ura$^+$ transformants should be different from the *PB*-flanking sequences in pPB[ura4]. To examine the *PB*-flanking sequences, we randomly picked 10 stable Ura$^+$ derivatives and performed inverse PCR using primers annealing to *PB* sequences close to the ITRs. For nine out of the ten transformants, a single distinct PCR product was obtained; and the other transformant gave rise to two distinct bands (data not shown). The sizes of these PCR products were different from each other, suggesting that *PB*-flanking sequences are likely to be unique sequences of fission yeast genome. Sequencing of the PCR products confirmed that *PB* indeed integrated into either chromosome 1 or 2 at 11 distinct sites (Supplementary Table S1). In each of these 11 mapped insertion events, the *PB* terminal sequences were next to sequences from the fission yeast genome rather than the plasmid backbone. The four terminal nucleotides were duplicated upon insertion and had a bias strongly favoring TTAA (10/11 TTAA; 1/10 TTAT). Together, these data indicated that the PBase-dependent *ura4*$^+$ integration events stemmed from transposition from the plasmid to the chromosomal DNA. All of the 11 insertion sites are located in intergenic regions, suggesting a possible bias against ORFs for *PB* transposition from a plasmid donor to chromosomes.

PB transposition in fission yeast leaves nearly no footprints

Typically, excision of *PB* from a donor site leaves no footprint and this has been tested true for all host systems examined thus far (21,22). In mammalian cells, it has been observed that *PB* excised from a donor site

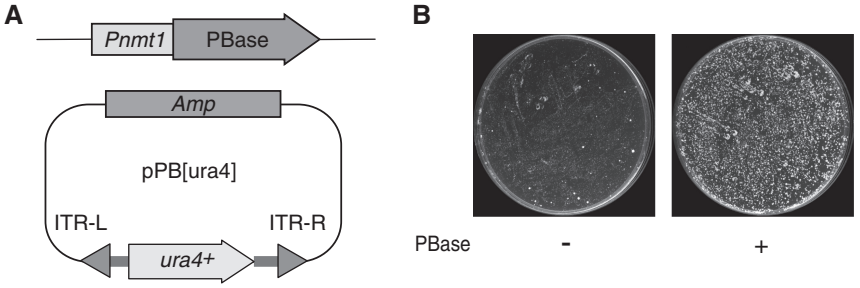

Figure 1. Transposition of *PB* in *S. pombe*. (**A**) A schematic view of the binary transposition system. pDUAL-PBase, a plasmid integrated into the *S. pombe* genome provided PBase under the control of the *nmt1* promoter. The donor plasmid pPB[ura4] provided a modified *PB* transposon lacking transposase but containing a *ura4*$^+$ selection marker. *Pnmt1*, promoter of *nmt1*. *Amp*, ampicillin-resistant cassette. ITR, inverted terminal repeat, is composed of a 13-bp terminal repeat and a 19-bp internal repeat. At the left end, ITR-L, two repeats are separated by a 3-bp spacer, and at the right end, ITR-R, by a 31-bp spacer. (**B**) Images of plates selecting for Ura$^+$ transformants of pPB[ura4]. When transformed with pPB[ura4], cells with PBase formed more colonies than those without on plates lacking uracil.

sometimes failed to re-insert into the genome (23,27). We took advantage of this phenomenon to collect *PB* excision events to test whether *PB* transposition leaves footprints in fission yeast. Because the *ura4*$^+$ marker can be counter-selected by FOA, cells that lose the *PB[ura4*$^+$*]* transposon after excision can be selected as colonies growing on FOA plates. DY2533 had *PB[ura4*$^+$*]* inserted 40 base pairs (bp) upstream of the *ade6* ORF (see 'Materials and Methods' section for strain construction) and this insertion prevented cells from growing on plates without adenine and rendered the colonies red on low adenine medium such as YE (Ade$^-$ phenotype) (Figure 2A). Upon the induction of PBase, cells were spread on YE+FOA plates and allowed to grow into colonies. We analyzed 49 FOA-resistant derivatives and found that 95.9% (47/49) were white (Ade$^+$) and 4.1% (2/49) were dark red (Ade$^-$). Therefore, vast majority of *PB* excision events were accompanied by restoration of a functional *ade6*$^+$ locus, consistent with a clean excision

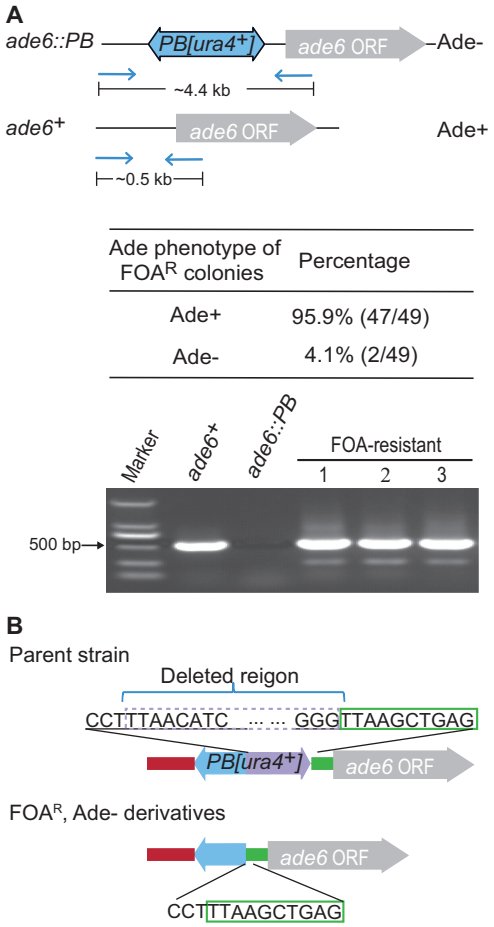

Figure 2. Excision of *PB* was nearly always precise. (**A**) More than 95% of the FOA-resistant derivatives of an *ade6::PB* strain were Ade$^+$ and had lost the *PB* sequence through precise excision. Representative examples of gel electrophoresis results of colony PCR products were shown. PCR was performed with primers flanking the insertion site (oligo 111 and 112). (**B**) In the two Ade$^-$ derivatives, a 2-kb PB sequence proximal to the *ade6* ORF was deleted (dashed rectangle). The deleted region was flanked by two TTAAs: one was at a *PB*-genome junction, and the other was inside the *ura4* ORF.

from the insertion site. From the 47 white colonies, we randomly picked 22 and confirmed by PCR that they all lacked the *PB* insertion (Figure 2A). We detected no deviation in the size of the PCR products from the expected 534 bp. This suggests that *PB* excision either left no footprint or ones that were too small to be discerned from the agarose gel. We sequenced the PCR products from four Ade$^+$ derivatives and found no base alternation around the excision site compared to the reference genome sequence, indicating that *PB* excision occurred in a precise fashion and left no footprint. In both Ade$^-$ derivatives (the FOA-resistant dark red colonies described above), we detected a deletion of the *ade6*-proximal region of the transposon (Figure 2B). Because this deletion removed part of the *ura4* marker, the cells were converted to Ura$^-$ without the loss of the entire *PB[ura4*$^+$*]*. Interestingly, the deleted sequence was flanked by two copies of *PB* preferred target motif, TTAA. Thus it is likely that two sequential transposition events might have generated this type of footprint (Supplementary Figure S1).

PB transposition can be monitored by a selectable excision marker

The precise excision of the *PB* transposon allowed us to develop a selectable marker to quantitatively monitor the excision events. In strain DY1432, *PB[ura4*$^+$*]* is located in the middle of the *arg6* ORF and consequently the cells are auxotrophic for arginine and prototrophic for uracil (Arg$^-$ Ura$^+$) (see 'Materials and Methods' section for strain construction). *PB* transposition from the *arg6* locus to another site will restore the function of *arg6*$^+$, thereby converting the cell from Arg$^-$ Ura$^+$ to Arg$^+$ Ura$^+$ (Figure 3A). Thus, the percentage of Arg$^+$ Ura$^+$ cells induced by PBase could represent the frequency of transposition events. Time-course studies conducted with DY1432 and two other strains with the same genotype showed that, the percentage of Arg$^+$ Ura$^+$ cells dramatically increased after PBase expression and peaked at ~10% around 36 h after the removal of thiamine (Figure 3B). This result suggests that *PB* integrated at a chromosomal site can undergo high frequency transposition, and *PB* inserted at an auxotrophic marker gene provides a useful means for detecting and enriching transposition events.

The copy number of *PB* remains constant among cells selected by the excision marker

A common problem with transposon-based mutagenesis is multiple insertions in the genome, which complicate identification of the mutation causing the phenotype. One reason we designed the *arg6* donor system that launches *PB* transposition from a chromosomal site is to avoid multiple insertions associated with launching the transposition from a multicopy episomal plasmid. However, even with a single copy chromosomal donor site, the copy number of a DNA transposon in individual cells can increase if transposition occurs in S or G2 phase of the cell cycle (28). In S or G2, a sister-chromatid can serve as the homologous recombination template, and DNA

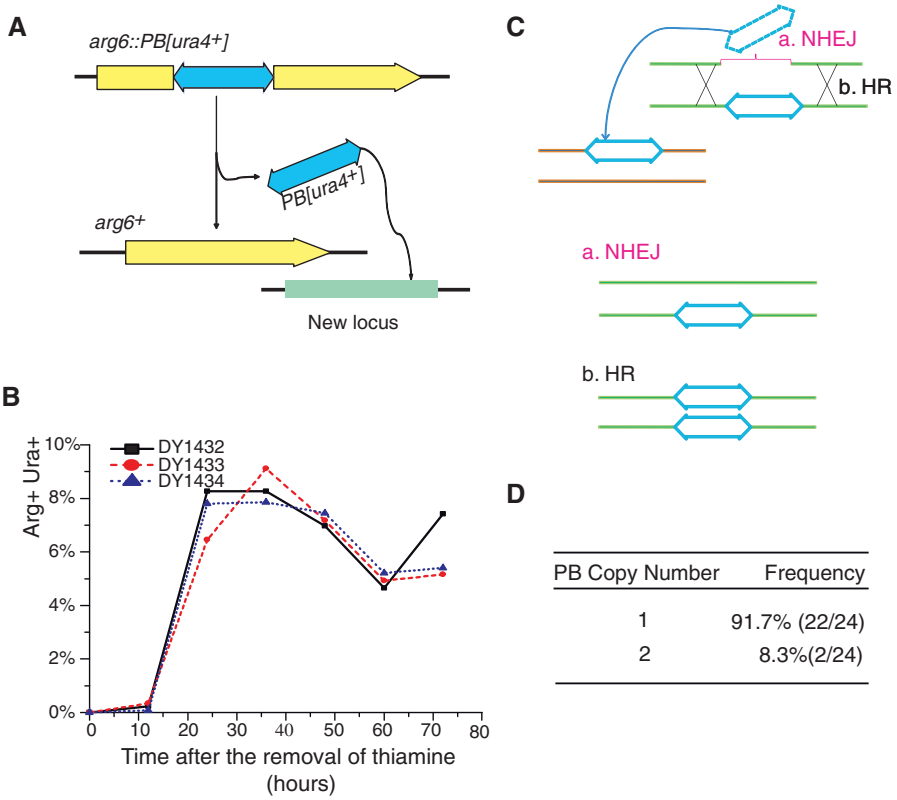

Figure 3. An excision marker allowed the transposition events to be monitored and enriched. (**A**) In the starting strain, a *PB* insertion in the *arg6* locus resulted in auxotrophy for arginine. Upon transposition, *PB* relocated from *arg6* to a new site, reverting cells from Arg$^-$ Ura$^+$ to Arg$^+$ Ura$^+$. (**B**) Transposition efficiency at the *arg6* locus. The percentage of Arg$^+$ Ura$^+$ cells was calculated as the number of colonies on EMM plates lacking arginine and uracil divided by the number of colonies on YES plates. Three independent strains with PBase-integration, DY1432, DY1433 and DY1434, were tested. (**C**) An illustration of how the *PB* copy number may be influenced by the choice of different DNA repair pathways. If transposition occurs at S or G2 phase, the repair pathway choice of non-homologous end joining (NHEJ) or homologous recombination (HR) could contribute to the copy number fluctuation. (**D**) The copy numbers of *PB* in Arg$^+$ Ura$^+$ derivatives were determined by monitoring the levels of *PB* versus *act1*$^+$ using qPCR (n = 24).

double-strand breaks formed upon *PB* transposition can be repaired by copying the *PB* from the sister, thus restoring the *PB*-containing sequence at the donor locus. This will lead to a net increase of the copy number of *PB* (Figure 3C). Besides inter-sister recombination, segregation of sister chromatids during mitosis can also lead to copy number change in the daughter cells (Supplementary Figure S2). In all these depicted schemes, the daughter cells with two copies of *PB* harbor one copy at the original donor site. We have indeed observed such type of copy number increase (J.-M. Zhang and L.-L. Du, unpublished observations). The use of a selectable excision marker like *arg6::PB* can in theory select against such events because only cells that lose the *PB* at the *arg6* donor site can grow on media lacking arginine. To analyze the extent of *PB* copy number change, we determined the copy number of *PB[ura4*$^+$*]* in the Arg$^+$ Ura$^+$ derivatives by quantitative PCR. After 36 h of PBase induction in DY1432, cells were spread on plates without arginine and uracil, allowing only Arg$^+$ Ura$^+$ cells to form colonies. Among the Arg$^+$ Ura$^+$ colonies examined, 91.7% (22/24) had only one copy of transposon, while 8.3% (2/24) contained two copies. This result suggested that if we only use transposition-induced Arg$^+$ Ura$^+$ cells for screening, the copy number of *PB* will not increase significantly, thus facilitating the utilization of *PB* as a mutagenesis tool in *S. pombe*.

Distribution of *PB* insertion sites in *S. pombe* genome

Ideally an effective mutagen should hit genes everywhere in the genome with similar frequency. To examine whether *PB* insertion events selected by the excision marker have a distribution bias, we applied Illumina sequencing technique to map the insertion sites of *PB* transposed from the *arg6* locus. From ~7 million raw sequence reads, we identified 33 218 independent insertion events that are supported by uniquely and perfectly matched reads. We counted *PB* insertions at the same position in opposite orientations as two independent insertions.

Consistent with our inverse PCR and Sanger sequencing analysis of 11 *PB* integration events (Supplementary Table S1), among deep sequencing-mapped insertions, the vast majority (96.7%) used TTAA as the target sequence, and most of the remaining ones used TTAA-like variant sequences such as TTAT and TTAG (Figure 4A).

Previous studies in insects, mouse, and *Plasmodium falciparum* suggested that, besides the nearly obligatory

A

Target	No. of events	Percentage
TTAA	32117	96.7%
TTAT	250	0.8%
ATAA	235	0.7%
CTAA	196	0.6%
TTAG	186	0.6%
ATAT	133	0.4%
CTAG	59	0.2%
Others	42	0.1%

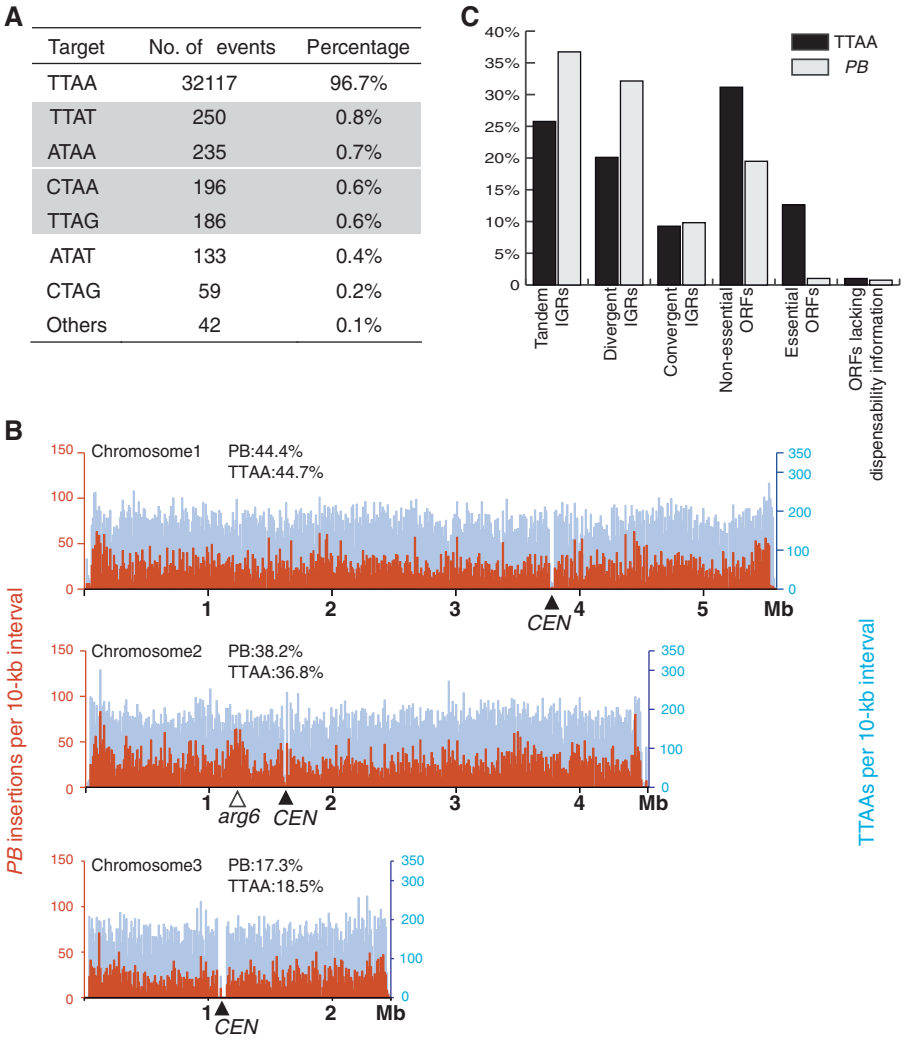

Figure 4. Profiling of *PB* insertion sites in *S. pombe* genome by Illumina sequencing. (**A**) Statistics of *PB* insertion target sequences. TTAA was the predominant target. Reverse-complement pairs (TTAT and ATAA, TTAG and CTAA) were highlighted with the same background. (**B**) Distribution of TTAA-targeting *PB* insertions along the three chromosomes. Each bar represents the number of independent *PB* insertion sites (red) or the number of reference TTAAs (blue) in a 10 kb-window. (**C**) Comparison of the genomic context of TTAA-targeting *PB* insertions and reference TTAAs. The proportions of insertion sites and reference TTAAs falling into different types of IGRs and ORFs are plotted. IGRs are classified into three types: divergent, tandem and convergent, based on the transcription orientations of the flanking genes. ORFs are classified based on whether their deletion mutants are lethal (essential), viable (non-essential) or with unknown phenotype (lacking dispensability information).

requirement for TTAA sequence, *PB* also has a slight preference for Ts in the five bases upstream of TTAA and As in the five bases downstream of TTAA (20,29,30). We observed a similar pattern in our deep sequencing-mapped insertions (Supplementary Figure S4).

To visualize the distribution of *PB* insertion sites in the genome, we plotted the numbers of *PB* insertion sites in 10-kb intervals along the three chromosomes (Figure 4B). We only plotted the insertions targeting TTAA because a great majority of *PB* insertion sites mapped to TTAA sites, and because we wanted to compare the insertion site distribution with a reference dataset of all the TTAA sequences whose flanking sequences can be uniquely mapped to the genome sequence. *PB* insertion site distribution among the three chromosomes largely correlates with TTAA distribution, with a slight bias favoring chromosome 2 where *PB* was launched from (38.2% for *PB* insertion sites versus 36.8% for reference TTAAs). There is a noticeable but moderate enrichment of *PB* insertion sites in a 100-kb region surrounding the *arg6* locus, suggesting a mild local hopping effect. By and large, *PB* insertion does not appear to strongly favor or avoid any particular regions of the fission yeast genome.

Seventy-nine percent of TTAA-targeting *PB* insertion sites are located in intergenic regions, compared to 55% for reference TTAA sites. The intergenic regions (IGRs) can be divided into three classes depending on the transcription directions of flanking ORFs: convergent IGRs, divergent IGRs and tandem IGRs. Among these three classes, we found that *PB* prefers tandem and divergent IGRs (Figure 4C).

Our insertion site mapping was done with haploid strains. Thus, the preference for intergenic regions can be at least partially explained by fitness loss resulted

from *PB* insertion into ORFs in the haploid cells. Consistent with this idea, when we analyzed the dispensability information of ORFs hit by *PB* (31), we found a much stronger bias against essential genes (1% of *PB* insertions are in essential genes versus 12.4% of reference TTAAs), compared to the non-essential ones (19.3% of *PB* insertions versus 31.2% of reference TTAAs) (Figure 4C).

PB insertion into ORFs may not always generate null alleles, as suggested by our observation of several hundred insertion sites inside of essential ORFs. We plotted the relative positions of insertion sites in essential and non-essential genes and found that, *PB* insertion in essential ORFs appeared to strongly favor the regions close to the stop codon, suggesting that most of these insertions resulted in functional gene products with small C-terminal truncations (Supplementary Figure S4). A similar but weaker distribution bias was observed for non-essential genes as well, suggesting there were fitness losses associated with *PB* insertions in non-essential genes.

For mutagenesis purpose, *PB* insertions outside of ORFs can be useful, as insertion into transcriptional regulatory sequences may result in hypomorphic alleles. Such hypomorphic alleles are particularly valuable for essential genes whose null alleles are inviable. When we analyzed the *PB* insertion sites located in the 400-bp regions upstream of ORFs and 400-bp regions downstream of ORFs, we noticed that *PB* insertion sites were found less frequently in regions immediately upstream of essential genes, indicating that insertion into 5′ flanking region can result in fitness loss (Supplementary Figure S5).

To examine whether gene expression level influences *PB* distribution, *PB* insertions in non-essential genes were tabulated according to the mRNA levels of their target genes (32). We did not observe a close relationship between *PB* insertion frequency and gene transcription level (Supplementary Figure S6).

Re-induction of transposition can reverse the phenotype caused by *PB* insertion

A necessary task in a transposon-based forward genetic screen is to verify whether the phenotype is caused by the transposon insertion or due to spontaneous mutations not related to the transposon. This can be addressed in our *PB* system by analyzing the linkage between the phenotype and the *ura4* maker, but it is time-consuming and cannot exclude the possibility that a spontaneous mutation had occurred near the inserted *PB*. Thus, we examined the feasibility of performing reversion analysis based on the 'no-footprints' feature of *PB*. The rationale is as follows: if the insertion of *PB* is responsible for the phenotype, precise excision of *PB* will abolish the phenotype; if the phenotype is not caused by *PB* insertion, excision of *PB* will not alter the phenotype. To obtain colonies derived from cells that had experienced an excision event, FOA counter-selection was used again.

DY3038 and DY3039 were isolated as TBZ-resistant mutants in a pilot genetic screen and each had a single copy of *PB* as determined by qPCR. In DY3038, it was found that *PB* remained at the *arg6* locus, i.e. no transposition had occurred. Thus, the TBZ resistance phenotype of DY3038 was likely due to a spontaneous mutation. As expected, the FOA-resistant derivatives of DY3038 were all as resistant to a high concentration of TBZ as the parent strain (Figure 5B). In contrast, DY3039 had *PB* inserted at a TTAA target site within the *klp6* gene whose null mutation is known to cause TBZ resistance (33). Consistently, all eight independent FOA-resistant derivatives of DY3039 lost the TBZ-resistance phenotype (Figure 5B). This demonstrates that reversion analysis is able to distinguish whether the mutant phenotype is caused by *PB* insertion.

One potential concern with this verification method is that when *PB* inserts into a non-TTAA site, its subsequent excision might leave a footprint, which then might cause the same phenotype as the *PB* insertion. This would give a false negative result, making the phenotype appear to be not associated with *PB* insertion. To address this concern, we analyzed two TTAG-targeted TBZ-resistant mutants and found no footprint left by the excision of *PB* from the TTAG sites and not surprisingly, the phenotype was reverted to that of the wild-type upon excision (Figure 5C and D).

Genetic screens with *PB*

Our general *PB*-based screening strategy is as follows: first, a strain containing the *arg6::PB* selectable excision marker and the integrated transposase gene is constructed; then after the induction of transposition, Arg^+ Ura^+ cells are enriched and further screened under certain conditions (Figure 6A). To investigate the feasibility of forward genetic screens with *PB* in *S. pombe*, we undertook two proof-of-principle screens: (i) for mutants resistant to the microtubule depolymerization drug, thiabendazole (TBZ); and (ii) for mutants that suppress the temperature-sensitive growth defect of *cdc25-22*.

In the screen for mutants resistant to 40 mg/l of TBZ, 3 OD600 units of mutagenized DY1434 cells were screened. The proportion of Arg^+ Ura^+ cells was ~6.3% as measured by plating assay. As 1 OD600 unit culture contains $\sim 10^7$ cells, we estimated that transposition occurred in $\sim 2 \times 10^6$ cells. In the end, we obtained 73 TBZ-resistant mutants.

Fission yeast Klp5 and Klp6 form a heterocomplex and are involved in the microtubule disassembly (33,34). Mutants harboring a deletion of either *klp5* or *klp6* have been reported to be resistant to high concentrations of TBZ (33). Because initial inverse PCR analysis suggested that these two genes were frequent hits of our screen, we used colony PCR to check whether these two genes were intact in the resistant clones. From the 73 TBZ-resistant mutants, we found 49 with *PB[ura4$^+$]* inserted in *klp5*, and 14 in *klp6* (Figure 6B). The junctions between *PB* and the fission yeast genome were then amplified and sequenced for each mutant. All insertions were located in the coding regions. There are 20 and 11 TTAA sites in the coding regions of *klp5*$^+$ and *klp6*$^+$, respectively. Of these, 60% (12/20) and 45.5% (5/11) of the potential insertion sites were targeted in our screen hits (Figure 6B).

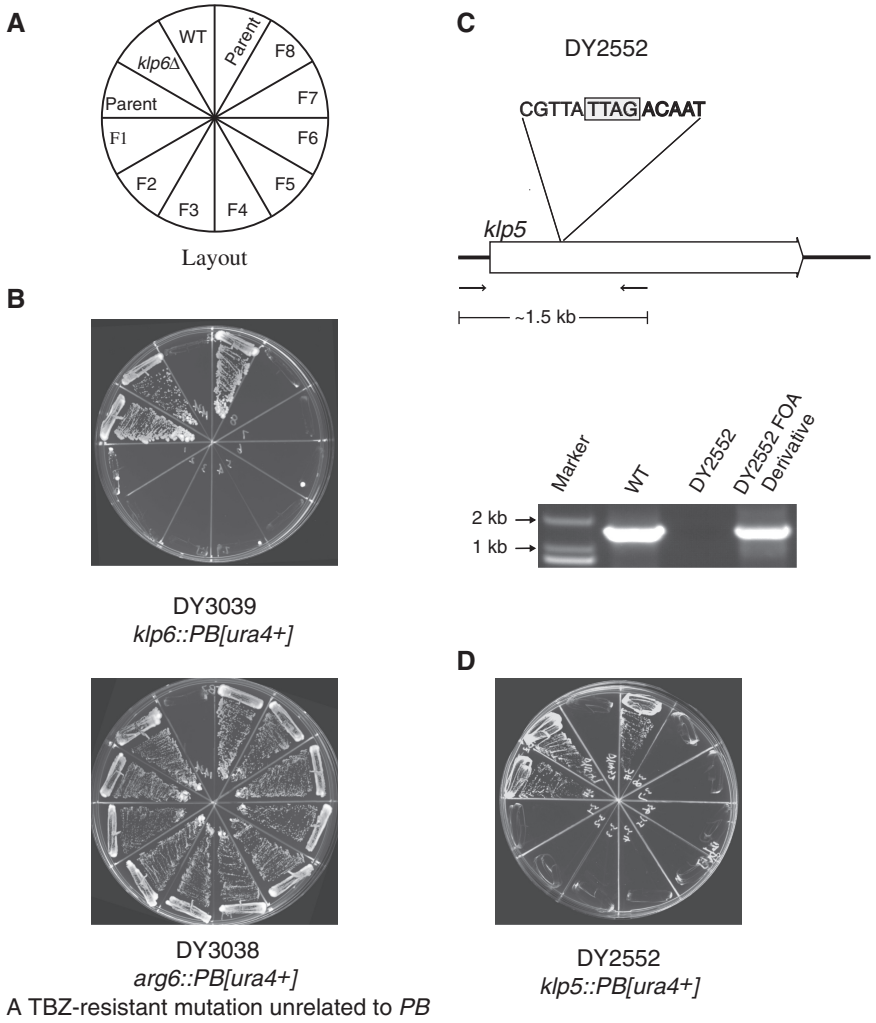

Figure 5. Reversion analysis. (**A**) A diagram of strain layout on TBZ plates. The TBZ-resistant parent strain and eight independent FOA-resistant derivatives (F1–F8) induced by remobilization of *PB* were streaked on plates containing 30 mg/l of TBZ. A *klp6Δ* deletion strain and a wild-type (WT) strain were also included as controls. (**B**) Phenotype differences of the FOA-resistant derivatives of two TBZ-resistant mutants isolated in a pilot *PB* mutagenesis screen. DY3039 had one copy of *PB* inserted at *klp6* and all its derivatives were as sensitive to TBZ as WT. In contrast, all the derivatives of DY3038, which contained a single copy of *PB* at *arg6*, were resistant to TBZ. The plates were photographed after 7 days at 30°C. (**C** and **D**) Excision of *PB* from non-TTAA sites was also precise. In a TBZ-resistant mutant DY2552, *PB* targeted a TTAG site in the *klp5* ORF. Both the colony PCR result using primers flanking the insertion site in *klp5* (C) and the reversion of TBZ resistance phenotype (D) suggested that no footprint was left after excision.

Besides TTAA, two different TTAG sites were also targeted in *klp5* ORF.

Apart from *klp5* and *klp6*, we also had 10 other mutants that might identify additional genes required for TBZ sensitivity. Through reversion analysis using the FOA selection of excision events, we determined that in seven of these mutants, the TBZ-resistant phenotype was due to spontaneous mutations rather than *PB* insertion. Thus, we performed inverse PCR to identify the *PB* insertion sites in the remaining three mutants and found that they all had an insertion at the only TTAA site in the ORF of *dam1* (Figure 6B). Fission yeast Dam1 is a subunit of the DASH complex required for proper chromosome segregation (35). Deletion of *dam1* makes cells hypersensitive to TBZ, thus the *PB* insertion allele is a gain-of-function mutation. The translational product of our *dam1::PB* allele consists of the N-terminal 102 amino acids of Dam1 followed by 31 amino acids derived from the *PB* terminal sequence (Figure 6B). The *dam1::PB* mutant showed similar resistance to TBZ as a *klp6* deletion strain (Figure 6C). It has previously been reported that *dam1* mutants with altered C-terminus, either in a truncated form or with two amino acid substitutions, are TBZ resistant (36,37).

Fission yeast Cdc25 dephosphorylates and activates cyclin-dependent kinase Cdc2, which is phosphorylated by the Wee1 kinase. Activation of Cdc2 is required for entry into mitosis. At 37°C, a temperature-sensitive mutant of *cdc25*, *cdc25-22*, is arrested at the G2/M stage. A saturated screen of *cdc25-22* suppressors by chemical mutagenesis showed that, besides very rare *cdc2* point mutations, the vast majority of extragenic

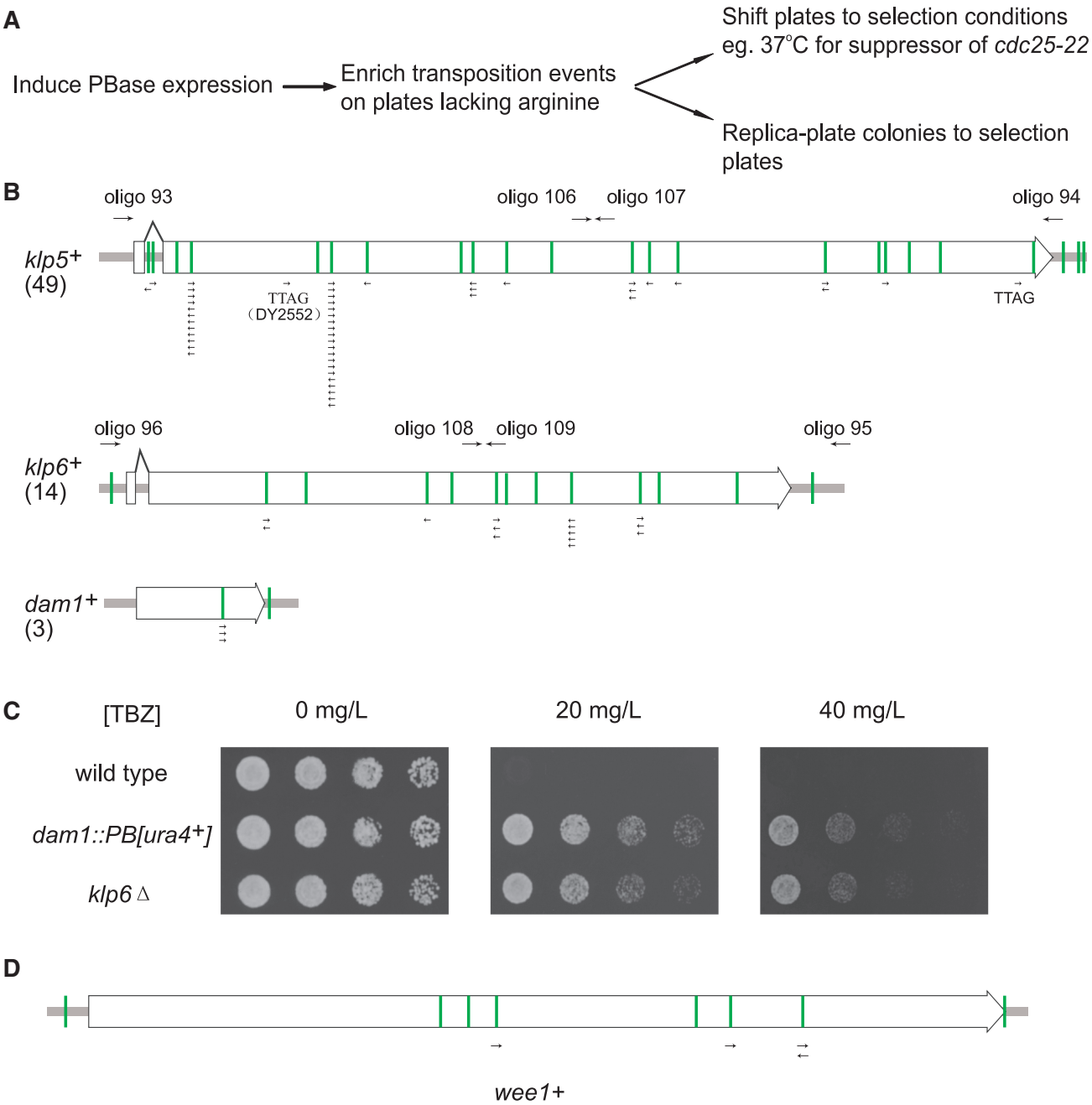

Figure 6. *PB*-mediated genetic screens. (**A**) Genetic screen strategy. Expression of PBase was induced in cells containing a single copy of *PB* at *arg6*. Next, transposition events were enriched by spreading cells on plates lacking arginine and uracil. Then, the cells were replica-plated to selection plates or shifted to screening conditions. (**B**) A schematic view of insertion sites of *PB* in *klp5*, *klp6* and *dam1* mutants isolated from the screen for TBZ-resistant mutants. The numbers in parentheses indicate the total numbers of mutants associated with each gene. Open boxes represent protein-coding regions. All TTAA sites are marked with green vertical lines. Primers used to check insertions by colony PCR are shown above the *klp5* and *klp6* ORFs as arrows. Smaller arrows below each gene denote *PB* insertions. The directions of the arrows indicate the directions of transcription of the *ura4*$^+$ marker in *PB*. Two insertions in *klp5* hit TTAG rather than TTAA. (B) Spot assay showed the TBZ resistance of an isolated *dam1* allele in comparison with the wild-type and the *klp6* null allele strains. Four-fold serial dilutions of cells were spotted on plates containing indicated concentrations of TBZ. The plates were photographed after 2 days at 30°C. (**C**) *wee1* was hit by *PB* in the *cdc25-22* suppressor screen at 37°C. Labels are the same as in (B).

suppressors were loss-of-function *wee1* alleles (38). We screened for suppressors of *cdc25-22* at the restrictive temperature and identified four *PB*-induced mutants. Each of them had one *PB* insertion in *wee1* ORF, covering 50% (3/6) of TTAA sites (Figure 6D).

DISCUSSION

In this study, we show that *PB* undergoes transposition in the presence of PBase in the fission yeast *S. pombe* and it can serve as an effective mutagenesis tool for genetic screens.

We developed a *PB*-based mutagenesis system for *S. pombe*. In this system, *PB* transposition is launched from an auxotrophic marker gene locus, thus allowing transposition events to be easily monitored and enriched. A major advantage of our system is that the copy number of the transposon stays at one in most of the mutagenized cells selected by the excision marker, thus avoiding the complication caused by multiple insertions. In addition, we took advantage of the precise nature of *PB* excision to implement an efficient reversion analysis procedure for verifying the causal relationship between the transposon insertion and the mutant phenotype.

A potential drawback of initiating transposition from a fixed chromosomal locus is the distribution bias caused by local hopping effect. Compared to other transposons used for mutagenesis, *PB* is known to have low tendency of local hopping (27). Our deep sequencing result showed that there was little chromosomal bias of *PB* insertions selected by the excision marker. The limited local hopping we observed is not likely to pose a problem for mutagenesis.

As shown for other organisms, TTAA is the preferred target site of *PB* in fission yeast while other TTAA-like 4-nt sequences could be targeted occasionally. There are ~110 000 TTAAs across the fission yeast chromosomal genome and ~40% of them are found in annotated genes (39). More than 98% of the fission yeast genes contain TTAA in their coding sequences and are susceptible to *PB* insertion (Supplementary Figure S7). Thus, it is theoretically possible to utilize *PB* to perform exhaustive screens of the fission yeast genome. Experimentally, from a mutant pool of 400 000 Arg^+ Ura^+ colonies, we detected *PB* insertions in 54% of the TTAA-containing ORFs using high-throughput sequencing (2647 out of 4914 genes). Insertions in the essential genes were severely under-represented, most likely due to insertion-caused lethality in haploid cells. For TTAA-containing non-essential ORFs, we found insertions in 66% of them (2306 out of 3468 genes). We believe this ratio is still an underestimate of the level of gene coverage that can be achieved by our system, because not all *PB* insertions isolated in our TBZ-resistant screen were detected by deep sequencing. For example, in *klp5*, only five of the 12 TTAAs identified as *PB* insertion sites in the TBZ screen were identified in sequencing-based profiling. The failure to detect all available insertion sites may be due to lower-than-saturation complexity of the mutant pool used for our sequencing analysis, and/or underrepresentation of certain sites caused by amplification bias of the PCR procedure.

We performed two proof-of-principle genetic screens to validate our system. In the screen for TBZ-resistant mutants, *klp5*, *klp6* and *dam1* mutants were found. Our literature search suggested that all the known mutants that can tolerate 40 mg/l of TBZ affect one of these three genes (33,34,36). Thus, our screen has identified all the expected genes. The number of Arg^+ Ura^+ cells screened (2×10^6) was about 20 times of the number of TTAA sites in the fission yeast genome. However, the numbers of TBZ-resistant isolates of the three hit genes were not as high as 20 times of the numbers of TTAA sites in these genes. Instead, for *klp5*, *klp6* and *dam1*, the numbers of isolates were 2.4, 1.3 and 3 times of the numbers of TTAA sites in their coding regions, respectively. This lower-than-expected recovery rate may be due to a *PB* insertion bias. We also observed uneven utilization of the TTAA sites within the same gene. For example, 20 insertion events were mapped to one TTAA site in *klp5* whereas no insertion was mapped to eight other TTAA sites in *klp5*. Most likely, there are both 'hot spots' and 'cold spots' among the TTAA sites in the same gene. To cover as many genes as possible, especially for the genes with fewer TTAA sites, it would be advisable to screen at least 10^6 Arg^+ Ura^+ cells using our system.

Based on current annotation, ~5000 genes are encoded by the *S. pombe* genome (39). A genome-wide haploid deletion library is commercially available from the Bioneer Corporation (http://pombe.bioneer.co.kr/). This library covers ~80% of non-essential genes and each mutant has two unique barcodes that can be monitored by microarray or high-throughput sequencing technique (31,40). This reverse genetics tool makes it possible to quickly identify genes responsible for a desired phenotype. However, a deletion library-based screen is not without limitations. For example, it would be difficult to carry out a screen in a genetic background different from that of the library because such an undertaking involves crossing the desired background into every single deletion strain in the library. In comparison, it is much easier to introduce the transposon elements into a specific genetic background to obtain a strain from which a transposon-based screen is initiated. Besides, all the mutations in the haploid deletion library are null alleles of non-essential genes, whereas different types of alleles can be expected from insertional mutagenesis, including hypermorphic alleles like the *dam1* mutants reported here as well as hypomorphic alleles of essential genes.

SUPPLEMENTARY DATA

Supplementary Data are available at NAR Online.

ACKNOWLEDGEMENTS

We thank Dr Xiaohui Wu at Fudan University for kindly providing the PB[SV40-neo] and the CMV-PBase plasmids. We thank Dr Meng-Qiu Dong for critically reading the article.

FUNDING

National Basic Research Program of China (973 Program; 2006CB806700); Chinese Ministry of Science and Technology 863 grant (2007AA02Z1A5). Funding for open access charges: Chinese Ministry of Science and Technology 863 grant.

Conflict of interest statement. None declared.

REFERENCES

1. Forsburg,S.L. (1999) The best yeast? *Trends Genet.*, **15**, 340–344.
2. Yanagida,M. (2002) The model unicellular eukaryote, Schizosaccharomyces pombe. *Genome Biol.*, **3**, comment2003.2001–comment2003.2004.
3. Wood,V., Gwilliam,R., Rajandream,M.A., Lyne,M., Lyne,R., Stewart,A., Sgouros,J., Peat,N., Hayles,J., Baker,S. *et al.* (2002) The genome sequence of Schizosaccharomyces pombe. *Nature*, **415**, 871–880.
4. Moreno,S., Klar,A. and Nurse,P. (1991) Molecular genetic analysis of fission yeast Schizosaccharomyces pombe. *Methods Enzymol.*, **194**, 795–823.
5. Irvine,D.V., Goto,D.B., Vaughn,M.W., Nakaseko,Y., McCombie,W.R., Yanagida,M. and Martienssen,R. (2009) Mapping epigenetic mutations in fission yeast using whole-genome next-generation sequencing. *Genome Res.*, **19**, 1077–1083.
6. Anders,A., Watt,S., Bahler,J. and Sawin,K.E. (2008) Improved tools for efficient mapping of fission yeast genes: identification of microtubule nucleation modifier mod22-1 as an allele of chromatin- remodelling factor gene swr1. *Yeast*, **25**, 913–925.
7. Chua,G., Taricani,L., Stangle,W. and Young,P.G. (2000) Insertional mutagenesis based on illegitimate recombination in Schizosaccharomyces pombe. *Nucleic Acids Res.*, **28**, E53.
8. Tanaka,K. and Russell,P. (2001) Mrc1 channels the DNA replication arrest signal to checkpoint kinase Cds1. *Nat. Cell Biol.*, **3**, 966–972.
9. Davidson,M.K., Young,N.P., Glick,G.G. and Wahls,W.P. (2004) Meiotic chromosome segregation mutants identified by insertional mutagenesis of fission yeast Schizosaccharomyces pombe; tandem-repeat, single-site integrations. *Nucleic Acids Res.*, **32**, 4400–4410.
10. Behrens,R., Hayles,J. and Nurse,P. (2000) Fission yeast retrotransposon Tf1 integration is targeted to 5′ ends of open reading frames. *Nucleic Acids Res.*, **28**, 4709–4716.
11. Singleton,T.L. and Levin,H.L. (2002) A long terminal repeat retrotransposon of fission yeast has strong preferences for specific sites of insertion. *Eukaryot. Cell*, **1**, 44–55.
12. Evertts,A.G., Plymire,C., Craig,N.L. and Levin,H.L. (2007) The hermes transposon of Musca domestica is an efficient tool for the mutagenesis of Schizosaccharomyces pombe. *Genetics*, **177**, 2519–2523.
13. Park,J.M., Evertts,A.G. and Levin,H.L. (2009) The Hermes transposon of Musca domestica and its use as a mutagen of Schizosaccharomyces pombe. *Methods*, **49**, 243–247.
14. Craig,N.L. (1997) Target site selection in transposition. *Annu. Rev. Biochem.*, **66**, 437–474.
15. Thibault,S.T., Singer,M.A., Miyazaki,W.Y., Milash,B., Dompe,N.A., Singh,C.M., Buchholz,R., Demsky,M., Fawcett,R., Francis-Lang,H.L. *et al.* (2004) A complementary transposon tool kit for Drosophila melanogaster using P and piggyBac. *Nat. Genet.*, **36**, 283–287.
16. Lobo,N., Fraser,T., Adams,J. and Fraser,M. (2006) Interplasmid transposition demonstrates piggyBac mobility in vertebrate species. *Genetica*, **128**, 347–357.
17. Cary,L.C., Goebel,M., Corsaro,B.G., Wang,H.G., Rosen,E. and Fraser,M.J. (1989) Transposon mutagenesis of baculoviruses: analysis of Trichoplusia ni transposon IFP2 insertions within the FP-locus of nuclear polyhedrosis viruses. *Virology*, **172**, 156–169.
18. Mitra,R., Fain-Thornton,J. and Craig,N.L. (2008) piggyBac can bypass DNA synthesis during cut and paste transposition. *Embo J.*, **27**, 1097–1109.
19. Handler,A.M. and Harrell,R.A. II (1999) Germline transformation of Drosophila melanogaster with the piggyBac transposon vector. *Insect. Mol. Biol.*, **8**, 449–457.
20. Ding,S., Wu,X., Li,G., Han,M., Zhuang,Y. and Xu,T. (2005) Efficient transposition of the piggyBac (PB) transposon in mammalian cells and mice. *Cell*, **122**, 473–483.
21. Fraser,M.J., Ciszczon,T., Elick,T. and Bauser,C. (1996) Precise excision of TTAA-specific lepidopteran transposons piggyBac (IFP2) and tagalong (TFP3) from the baculovirus genome in cell lines from two species of Lepidoptera. *Insect. Mol. Biol.*, **5**, 141–151.
22. Elick,T.A., Bauser,C.A. and Fraser,M.J. (1996) Excision of the piggyBac transposable element in vitro is a precise event that is enhanced by the expression of its encoded transposase. *Genetica*, **98**, 33–41.
23. Wang,W., Bradley,A. and Huang,Y. (2009) A piggyBac transposon-based genome-wide library of insertionally mutated Blm-deficient murine ES cells. *Genome Res.*, **19**, 667–673.
24. Matsuyama,A., Arai,R., Yashiroda,Y., Shirai,A., Kamata,A., Sekido,S., Kobayashi,Y., Hashimoto,A., Hamamoto,M., Hiraoka,Y. *et al.* (2006) ORFeome cloning and global analysis of protein localization in the fission yeast Schizosaccharomyces pombe. *Nat. Biotechnol.*, **24**, 841–847.
25. Livak,K.J. and Schmittgen,T.D. (2001) Analysis of relative gene expression data using real-time quantitative PCR and the 2(-Delta Delta C(T)) Method. *Methods*, **25**, 402–408.
26. Langmead,B., Trapnell,C., Pop,M. and Salzberg,S.L. (2009) Ultrafast and memory-efficient alignment of short DNA sequences to the human genome. *Genome Biol.*, **10**, R25.
27. Wang,W., Lin,C., Lu,D., Ning,Z., Cox,T., Melvin,D., Wang,X., Bradley,A. and Liu,P. (2008) Chromosomal transposition of PiggyBac in mouse embryonic stem cells. *Proc. Natl Acad. Sci. USA*, **105**, 9290–9295.
28. Engels,W.R., Johnson-Schlitz,D.M., Eggleston,W.B. and Sved,J. (1990) High-frequency P element loss in Drosophila is homolog dependent. *Cell*, **62**, 515–525.
29. Balu,B., Chauhan,C., Maher,S.P., Shoue,D.A., Kissinger,J.C., Fraser,M.J. and Adams,J.H. (2009) piggyBac is an effective tool for functional analysis of the Plasmodium falciparum genome. *BMC Microbiol.*, **9**, 83.
30. Li,X., Harrell,R.A., Handler,A.M., Beam,T., Hennessy,K. and Fraser,M.J. (2005) piggyBac internal sequences are necessary for efficient transformation of target genomes. *Insect Mol. Biol.*, **14**, 17–30.
31. Kim,D.U., Hayles,J., Kim,D., Wood,V., Park,H.O., Won,M., Yoo,H.S., Duhig,T., Nam,M., Palmer,G. *et al.* (2010) Analysis of a genome-wide set of gene deletions in the fission yeast Schizosaccharomyces pombe. *Nat. Biotechnol.*, **28**, 617–623.
32. Lackner,D.H., Beilharz,T.H., Marguerat,S., Mata,J., Watt,S., Schubert,F., Preiss,T. and Bahler,J. (2007) A network of multiple regulatory layers shapes gene expression in fission yeast. *Mol. Cell*, **26**, 145–155.
33. West,R.R., Malmstrom,T., Troxell,C.L. and McIntosh,J.R. (2001) Two related kinesins, klp5+ and klp6+, foster microtubule disassembly and are required for meiosis in fission yeast. *Mol. Biol. Cell*, **12**, 3919–3932.
34. Garcia,M.A., Koonrugsa,N. and Toda,T. (2002) Two kinesin-like Kin I family proteins in fission yeast regulate the establishment of metaphase and the onset of anaphase A. *Curr. Biol.*, **12**, 610–621.
35. Sanchez-Perez,I., Renwick,S.J., Crawley,K., Karig,I., Buck,V., Meadows,J.C., Franco-Sanchez,A., Fleig,U., Toda,T. and Millar,J.B.A. (2005) The DASH complex and Klp5/Klp6 kinesin coordinate bipolar chromosome attachment in fission yeast. *EMBO J.*, **24**, 2931–2943.
36. Griffiths,K., Masuda,H., Dhut,S. and Toda,T. (2008) Fission yeast dam1-A8 mutant is resistant to and rescued by an anti-microtubule agent. *Biochem. Biophys. Res. Commun.*, **368**, 670–676.
37. Sanchez-Perez,I., Renwick,S.J., Crawley,K., Karig,I., Buck,V., Meadows,J.C., Franco-Sanchez,A., Fleig,U., Toda,T. and Millar,J.B.A. (2005) The DASH complex and Klp5/Klp6 kinesin coordinate bipolar chromosome attachment in fission yeast. *Embo J.*, **24**, 2931–2943.
38. Fantes,P.A. (1981) Isolation of cell size mutants of a fission yeast by a new selective method: characterization of mutants and implications for division control mechanisms. *J. Bacteriol.*, **146**, 746–754.
39. Wood,V., Gwilliam,R., Rajandream,M.A., Lyne,M., Lyne,R., Stewart,A., Sgouros,J., Peat,N., Hayles,J., Baker,S. *et al.* (2002) The genome sequence of Schizosaccharomyces pombe. *Nature*, **415**, 871–880.
40. Han,T.X., Xu,X.Y., Zhang,M.J., Peng,X. and Du,L.L. (2010) Global fitness profiling of fission yeast deletion strains by barcode sequencing. *Genome Biol.*, **11**, R60.